

Map Equation Centrality: A Community-Aware Centrality Score Based on the Map Equation

Christopher Blöcker*

Integrated Science Lab, Department of Physics, Umeå University, SE-901 87 Umeå, Sweden

Juan Carlos Nieves†

Department of Computing Science, Umeå University, SE-901 87 Umeå, Sweden

Martin Rosvall‡

Integrated Science Lab, Department of Physics, Umeå University, SE-901 87 Umeå, Sweden

(Dated: February 1, 2022)

To measure node importance, network scientists employ centrality scores that typically take a microscopic or macroscopic perspective, relying on node features or global network structure. However, traditional centrality measures, such as degree centrality and PageRank, neglect the community structure found in real-world networks. To study node importance based on network flows from a mesoscopic perspective, we analytically derive a community-aware information-theoretic centrality score based on the coding principles behind the map equation: map equation centrality. Map equation centrality measures how much further we can compress the network’s modular description by not coding for random walker transitions to the respective node, using an adapted coding scheme. It can be determined from the local network context alone because changes to the coding scheme affect only the node’s module. Applied to synthetic and real-world networks, we highlight how our approach enables a more fine-grained differentiation between nodes than node-local or network-global measures. Map equation centrality tends to outperform other community-aware centrality measures.

I. INTRODUCTION

Networks are simple yet powerful representations of how things connect: the world wide web captures connections between websites, and social networks describe relationships between persons. So-called centrality measures determine node importance and enable us to rank nodes, compare them with each other, and find the most important ones. Real-world applications are manifold and include identifying the most popular websites, which components in an infrastructure network have the most impact when they fail, and who drives disease spreading in a social network.

Classical centrality measures consider node importance on a microscopic scale at the node level or on a macroscopic scale at the network level. For example, degree centrality defines a node’s importance as its degree, and betweenness centrality calculates node importance as the number of shortest paths that pass through it [1]. Eigenvector centrality-based measures, such as Katz centrality [2] and PageRank [3], implement a reputation system and derive a node’s importance from how important its neighbours are, leading to a system of recursive equations. However, real-world networks often exhibit community structure. Loosely speaking, they contain groups of nodes, so-called communities, with more connections

within groups than between. Classical centrality measures neglect the mesoscopic scale of communities and cannot distinguish between nodes with the same features or nodes embedded in similar network regions. For example, degree centrality assigns the same score to same-degree nodes, and PageRank cannot distinguish between nodes receiving the same amount of support.

To address this issue, network scientists have developed community-aware centrality scores that typically define node importance in terms of intra-community and inter-community link patterns. For example, community-based betweenness centrality considers only shortest paths with endpoints in different communities [4]. Community hub-bridge calculates a node’s importance as the sum of its intra-community and inter-community links, weighted by the size of the node’s community and the number of communities it connects to, respectively [5]. Community-based centrality determines a node’s importance as the number of connections it has to other communities, weighted by the communities’ relative sizes [6]. Other approaches include defining a generic framework that operates on top of classical centrality measures to retrofit them with community-awareness [7], or deriving centrality scores from community-detection methods. Recently, modularity vitality has been proposed [8] based on the community-detection approach known as modularity [9]. Deriving the community-aware centrality score from a community-detection approach provides clarity and precision.

Here we focus on the information-theoretic community-detection method known as the map equation [10] and derive a community-aware centrality

* christopher.blocker@umu.se

† juan.carlos.nieves@umu.se

‡ martin.rosvall@umu.se

score analytically: *map equation centrality*. Using small synthetic networks, we highlight how map equation centrality exploits community structure to distinguish between nodes where classical centrality measures fail. To evaluate the performance of map equation centrality, we apply it to empirical networks to identify influential nodes. Following established procedures for evaluating centrality scores, we contrast our predictions with the spreading power of nodes obtained from simulations of an SIR disease-spreading model [5, 11]. For comparison, we include other community-aware centrality measures in our evaluation and find that map equation centrality tends to outperform those baseline measures.

II. THE MAP EQUATION FRAMEWORK

The map equation [10] is a flow-based information-theoretic objective function for community detection. It takes a network $G = (V, E, \delta)$, possibly weighted and/or directed, and a partition \mathbf{M} of the network's nodes into modules as input, and measures how well the partition captures the network's community structure. Here, V is the set of nodes, $E \subseteq V \times V$ is the set of links, and $\delta: E \rightarrow \mathbb{R}^+$ is a function that assigns weights to the links. A partition \mathbf{M} is a split of the graph's nodes into disjoint, possibly nested sets.

Conceptually, the map equation models network flow with a random walk on the network and calculates how many bits are required, on average, to encode one random-walker step. To explain the inner workings of the map equation, we consider a communication game where the sender updates the receiver about the location of a random walker on a network. We assume that, when at node u , the probability that the random walker chooses an outgoing edge $e = (u, v) \in E$ is proportional to the edge's weight, $\delta(e)$.

In the simplest case, when there is only one module that contains all nodes, we assign unique codewords to the nodes according to a Huffman code based on the nodes' visit rates at ergodicity. We refer to such a partition as the one-level partition and denote it as \mathbf{M}_1 . When the random walker takes a step, the sender communicates one codeword to the receiver (Fig. 1a). According to Shannon's source coding theorem [12], the lower bound for the per-step codelength, L , is precisely the entropy of the nodes' visit rates,

$$L(G, \mathbf{M}_1) = H(P) = - \sum_{u \in V} p_u \log_2 p_u, \quad (1)$$

where H is the Shannon entropy, P is the set of node visit rates, and p_u is the visit rate of node u .

In undirected graphs, we calculate the node visit rates analytically as $p_u = \frac{s_u}{\sum_{v \in V} s_v}$, where $s_u = \sum_{v \in V} \delta((u, v))$ is the strength of node u . In directed graphs, we obtain the visit rates numerically as the stationary distribution of a random walk on the network. The Perron-Frobenius

theorem guarantees the existence of such an ergodic distribution in strongly connected graphs; to ensure ergodicity in weakly-connected graphs, there are different options. PageRank relaxes these dynamics by introducing uniform node teleportation, letting the random walker teleport to a node selected uniformly at random at some small rate [3], introducing a teleportation parameter. To reduce the effect of this parameter, here we rely on so-called unrecorded link teleportation [13], a similar approach where the random walker teleports, at some small rate, to links proportionally to their weight.

In networks with community structure, we can achieve shorter codelengths than with the one-level partition. Splitting the nodes into modules allows us to assign unique codewords within modules, and re-use codewords across modules. However, we need to pay for this by encoding transitions between modules: we introduce one designated exit codeword per module, as well as an index-level codebook for encoding transitions into modules. Now, the sender communicates one codeword for transitions within modules, and three codewords for transitions between modules, that is one module exit codeword from the old module codebook, one module entry codeword from the index-level codebook, and one codeword from the new module codebook to visit a node in the new module (Fig. 1). The codelength for such a two-level map is given by the sum of the index-level entropy and the module-level entropies, weighted by the rate at which each codebook is used,

$$L(G, \mathbf{M}) = qH(Q) + \sum_{\mathbf{m} \in \mathbf{M}} p_{\mathbf{m}}H(P_{\mathbf{m}}). \quad (2)$$

Here, $P_{\mathbf{m}} = \{p_u \mid u \in \mathbf{m}\} \cup \{m_{\text{exit}}\}$ is the set of node visit rates for module \mathbf{m} , including the module exit rate for module \mathbf{m} , m_{exit} , and $p_{\mathbf{m}} = \sum_{p \in P_{\mathbf{m}}} p$ is the rate at which the sender uses the codebook for module \mathbf{m} . $Q = \{m_{\text{enter}} \mid \mathbf{m} \in \mathbf{M}\}$ is the set of module entry rates, and $q = \sum_{q_{\mathbf{m}} \in Q} q_{\mathbf{m}}$ is the rate at which the sender uses the index-level codebook.

When a partition reflects the structure of the network well and groups those nodes together where the random walker stays for a longer time, transitions between modules occur at a low frequency, overall compressing the average per-step codelength. Thus, finding the optimal partition according to the map equation becomes a search problem. Through recursion, we can generalise this approach to partitions nested at arbitrary depth and reduce the codelength even further in networks with hierarchical community structure.

III. MAP EQUATION CENTRALITY

To define our community-aware centrality score, map equation centrality, we take inspiration from the concept of network vitality. Given a function f that operates on graphs and calculates a numerical value, the vitality

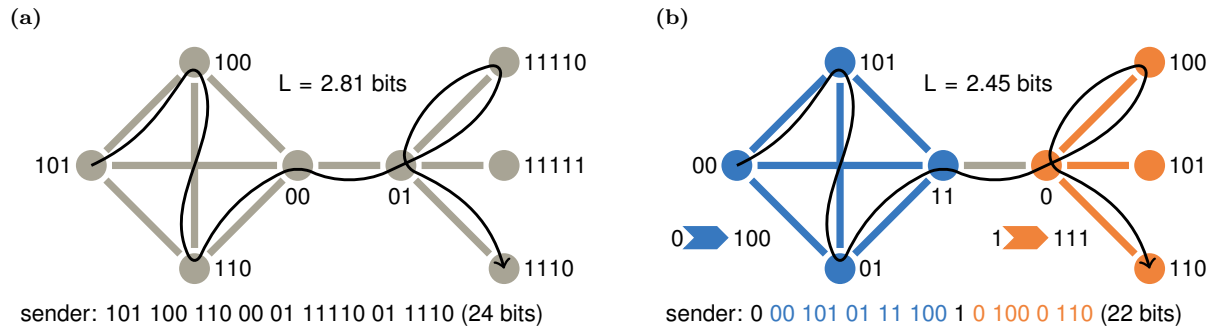


Figure 1: A communication game on a graph where colours indicate module assignments and node labels show codewords. The black trace shows a possible node sequence during a random walk; the corresponding sequence of codewords to describe the walk is shown in the bottom. The average per-step codeword length is shown as L . **(a)** The one-level partition where all nodes are in the same module and there is only one codebook. **(b)** Nodes are split into two modules with one codebook per module and an additional index-level codebook, indicated by coloured arrows. Module entry and exit codewords are shown on the left and right of the arrows, respectively. The codeword length L is reduced because the partition captures those areas where the random walker tends to stay for a longer time.

$\mu(G, u)$ with respect to a node u is defined as

$$\mu(G, u) = f(G) - f(G - \{u\}), \quad (3)$$

where $G - \{u\}$ denotes G with u removed [1]. But because removing a node and its incident edges from the graph would disrupt the graph's community structure and change the node visit rates, instead, we keep the graph unchanged and only omit u when describing the community structure – we call this *silencing a node*.

To explain what silencing a node means, we consider the communication game again. When the random walker visits a silenced node u , the sender does not communicate the codeword for visiting u to the receiver (Fig. 2a). But this is inefficient because node u has a codeword that is never used, that is, the sender uses more bits than necessary to describe the random walk. Instead, we can design a new coding scheme without assigning a codeword to u and, thereby, compress the description of the random walk (Fig. 2b). Node u 's contribution to the random walk's description length is the difference between the default, inefficient code—we call it L^u —and the updated, efficient code—we call it L^{u*} . To reflect these ideas, we modify Eq. 3 to take a partition M and the two ways to encode it into account, and define map equation centrality,

$$\lambda(G, M, u) = L^u(G, M) - L^{u*}(G, M). \quad (4)$$

Essentially, map equation centrality conforms to the principle of vitality, but instead of measuring the difference between the values for two networks, we measure the difference between two descriptions of the same network. Effectively, this is the marginal harm for a modular network description that a node causes to the rest of the nodes by its existence. We derive expressions for L^u and L^{u*} from the map equation, and, for clarity, begin with one-level partitions, then moving on to two-level and hierarchical partitions.

First, we consider the case where we use the old coding scheme. We obtain the codeword length resulting from silencing u from Eq. 1 by removing u from the summation,

$$L^u(G, M_1) = - \sum_{v \in V, v \neq u} p_v \log_2 p_v. \quad (5)$$

Designing a new coding scheme without a codeword for u changes the codeword lengths for the rest of the nodes. Before, the codeword length for some node v was given by its visit rate as $\log_2 p_v$, but now that u does not receive a codeword anymore, we need to re-normalise accordingly. The new codeword length for node $v \neq u$ is $\log_2 \frac{p_v}{1-p_u}$, and for u it is zero, resulting in a codeword length of

$$L^{u*}(G, M_1) = - \sum_{v \in V, v \neq u} p_v \log_2 \frac{p_v}{1-p_u}. \quad (6)$$

Plugging Eq. 5 and Eq. 6 into Eq. 4, we get u 's contribution to the codeword length in the one-level partition M_1 ,

$$\begin{aligned} \lambda(G, M_1, u) &= L^u(G, M_1) - L^{u*}(G, M_1) \\ &= -(1-p_u) \log_2 (1-p_u). \end{aligned} \quad (7)$$

We move on to derive the same quantities for two-level partitions M . Again, we begin by considering the resulting codeword length when silencing node u but using the old coding scheme. Then, we design a new coding scheme that does not assign a codeword to u and calculate the difference between the two coding schemes to obtain u 's contribution. For clearer derivations, we distinguish explicitly between m_u , the module that contains u , and the rest of the modules by rewriting the map equation

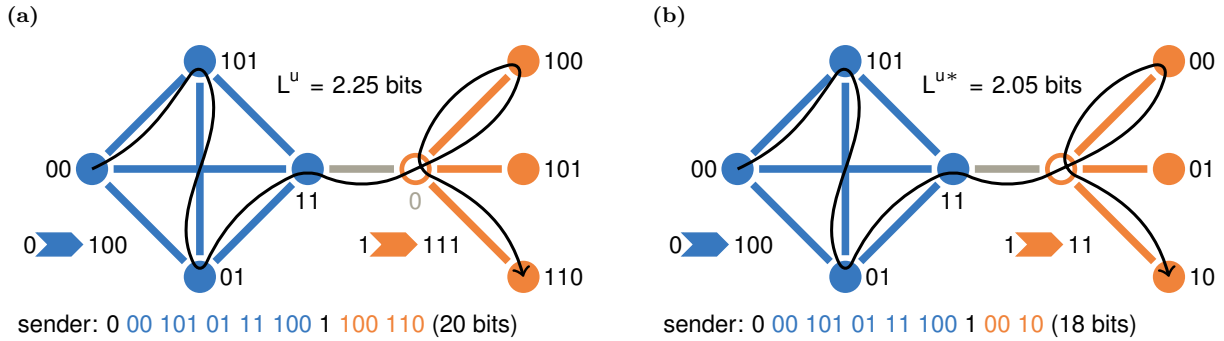


Figure 2: Two options for describing a random walk when a node is silenced, with the silenced node shown as a ring.

(a) Using the same code as before: when the random walker visits the silenced node, the sender does not use the corresponding node-visit codeword. (b) Designing a new code: the silenced node does not receive a codeword and visits to that node cannot be encoded. However, the sender communicates module entries through the silenced node.

(Eq. 2),

$$L(G, M) = qH(Q) + \sum_{m \in M} p_m H(P_m)$$

$$= \overbrace{qH(Q)}^{\text{index level}} + \overbrace{\sum_{m \in M, m \neq m_u} p_m H(P_m)}^{\text{modules without } u} - \overbrace{\sum_{p \in P_{m_u}} p \log_2 \frac{p}{p_{m_u}}}^{\text{module with } u}. \quad (8)$$

From Eq. 8, it becomes clear that silencing node u in a two-level partition only affects the module that contains u because a codeword for u only exists in the context of m_u , but not in other modules. The codeword for a two-level partition M , using the old coding scheme while u is silenced is

$$L^u(G, M) = \overbrace{qH(Q)}^{\text{index level}} + \overbrace{\sum_{m \in M, m \neq m_u} p_m H(P_m)}^{\text{modules without } u} - \overbrace{\sum_{p \in P_{m_u} \setminus \{p_u\}} p \log_2 \frac{p}{p_{m_u}}}^{\text{module with } u}. \quad (9)$$

Because of the modular structure of the coding scheme, when designing a new code, only codewords for nodes in module m_u are affected while other modules and the index level remain unaffected. The new codebook usage rate for module m_u is $p_{m_u} - p_u$, which is also the term we use for re-normalising the node visit rates for nodes in m_u . That is, the new rate at which the codeword for $v \in m_u$ with $v \neq u$ is used is $\frac{p_v}{p_{m_u} - p_u}$, and the module exit codeword is used at rate $\frac{p_{m_u \text{ exit}}}{p_{m_u} - p_u}$. The new codeword for M is

$$L^{u*}(G, M) = \overbrace{qH(Q)}^{\text{index level}} + \overbrace{\sum_{m \in M, m \neq m_u} p_m H(P_m)}^{\text{modules without } u} - \overbrace{\sum_{p \in P_{m_u} \setminus \{p_u\}} p \log_2 \frac{p}{p_{m_u} - p_u}}^{\text{module with } u}. \quad (10)$$

Plugging Eq. 9 and Eq. 10 into Eq. 4, we get u 's contribution to the two-level codeword where the terms for

the index level and those modules that do not contain u cancel out,

$$\lambda(G, M, u) = L^u(G, M) - L^{u*}(G, M)$$

$$= -(p_{m_u} - p_u) \log_2 \frac{p_{m_u} - p_u}{p_{m_u}} \quad (11)$$

For the one-level partition M_1 , the expression in Eq. 11 reduces to Eq. 7 because all nodes are in the same module and, consequently, $p_{m_u} = 1$.

Through recursion, we can extend map equation centrality to hierarchical partitions with more than two levels. In fact, since silencing a node u only affects module m_u , Eq. 11 can be used to calculate centralities for nodes in modules that are nested deeper in the module hierarchy of a graph. Further, we can extend map equation centrality to silencing a set of nodes by adjusting Eq. 9 and Eq. 10 (see appendix A), leading to

$$\lambda(G, M, U) = - \sum_{m \in M, m \cap U \neq \emptyset} (p_m - p_{m \cap U}) \log_2 \frac{p_m - p_{m \cap U}}{p_m}. \quad (12)$$

Here, U is the set of nodes that are silenced, and $p_{m \cap U} = \sum_{u \in m \cap U} p_u$ is the sum of visit rates for the silenced nodes in module m .

Map equation centrality relates to the Kullback-Leibler divergence, also known as relative entropy, and defined as $D_{KL}(P||Q) = - \sum_{x \in X} p(x) \log_2 \frac{q(x)}{p(x)}$, where X is a set of events, and P and Q are probability distributions over X . The KL divergence quantifies the expected number of extra bits that are required to encode a sequence of events with true distribution P , assuming that we use a code optimised for Q . In this light, the importance of a node u is the Kullback-Leibler divergence between encoding visits in module m_u with true codebook usage rate p_{m_u} and silencing u , resulting in a new codebook usage rate after silencing of $p_{m_u} - p_u$. Because no other modules than m_u contribute to our score, u 's importance under map equation centrality is fully determined by its own visit rate p_u and its modular context through p_{m_u} .

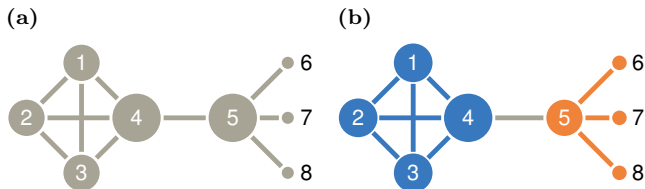


Figure 3: Illustration of the centrality scores from Table I. Node colours indicate community assignments, node diameter is proportional to (a) degree centrality and PageRank without teleportation, and (b) map equation centrality.

IV. APPLICATION TO SYNTHETIC AND EMPIRICAL NETWORKS

We have implemented map equation centrality in Infomap, a fast and greedy optimisation algorithm for the map equation [14] with an open source implementation [15]. To evaluate map equation centrality, we apply it to synthetic and empirical networks. First, using a small synthetic network, we highlight how map equation centrality addresses the issue that traditional centrality scores cannot distinguish between same-feature nodes. Second, using two synthetic, networks with highly regular structure but without community structure, we point out the limitations of map equation centrality. Third, we evaluate the performance of map equation centrality, alongside other community-aware centrality scores, on a set of empirical social networks.

A. Map equation centrality discerns same-feature nodes

We use a small, undirected network with eight nodes and ten links (Fig. 3), and use Infomap to calculate map equation centrality scores for its nodes (Table I). The optimal way to partition the network, by design and recovered by Infomap, is to group the nodes into two communities as indicated by colours (Fig. 3b).

We find that neither degree centrality, nor PageRank, nor map equation centrality when based on the one-level partition M_1 can distinguish between nodes with the same degree (Fig. 3a, Table I). This is because using M_1 turns map equation centrality into a global approach, ignoring the network’s mesoscopic community structure. However, when using the two-level partition M_{opt} (Fig. 3b), map equation centrality distinguishes between same-degree nodes that are embedded in different modules, such as nodes 4 and 5, while same-degree nodes in the same module remain indistinguishable, such as nodes 1, 2, and 3, or nodes 6, 7, and 8, respectively (Fig. 3b, Table I). In some cases, map equation centrality reverses the ranking of nodes compared to PageRank: while PageRank ranks node 5 higher than nodes 1, 2, and

Table I: Centrality scores for the synthetic network, rounded to two decimal places: degree centrality, DC, PageRank without teleportation, and map equation centrality, λ , for the one-level partition M_1 and the optimal partition M_{opt} , shown in (Fig. 3).

Node	DC	PageRank	$\lambda(M_1)$	$\lambda(M_{opt})$
1	3	0.15	0.20	0.19
2	3	0.15	0.20	0.19
3	3	0.15	0.20	0.19
4	4	0.20	0.26	0.24
5	4	0.20	0.26	0.18
6	1	0.05	0.07	0.07
7	1	0.05	0.07	0.07
8	1	0.05	0.07	0.07

3, map equation centrality ranks nodes 1, 2, and 3 higher than node 5 under M_{opt} . We explain this by interpreting Eq. 11: the importance of a node u is determined by its visit rate, p_u , as well as the codebook usage rate of its module, p_{m_u} , that is, modules with a higher codebook usage rate boost the importance of their member nodes to a higher degree than modules with a lower codebook usage rate.

B. Dependence on Partition Quality

The performance of map equation centrality, and community-aware centrality scores in general, depends on the quality of the used networks partition. Consider two networks with highly regular structure: a ring (Fig. 4a), and a grid (Fig. 4b). Because of the regularity in these two networks, we expect that in the ring network, all nodes should have the same centrality score while in the grid network all inner nodes, corner nodes, and remaining edge nodes, respectively, should receive the same score. However, community detection methods, including the map equation, are known to detect spurious communities in such networks due to the so-called resolution limit [16, 17]. Such spurious communities lead to different scores than we expect, resulting in different scores for nodes that should be equal. For example, in the ring network, Infomap detects three communities, two with three nodes, and one with four nodes (Fig. 4a). Since all nodes have the same visit rate but one of the module is larger with a higher codebook usage rate, map equation centrality assigns higher importance to the nodes in the larger module. In the 5×5 grid networks, Infomap detects four communities with different sizes (Fig. 4b), leading to small centrality differences for nodes in corresponding positions depending on the size of their community. Consequently, while partitions that reflect a network’s structure well support community-aware centrality scores in discerning nodes that are otherwise indistinguishable, spurious communities can cause misleading

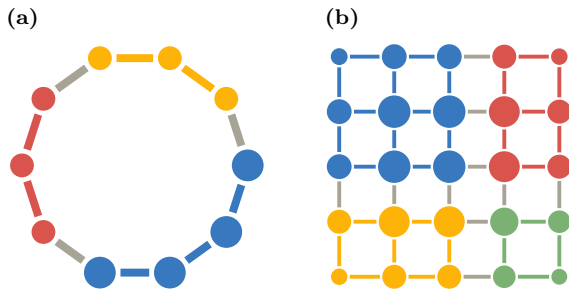


Figure 4: Two networks without community structure where community-detection methods are known to erroneously detect communities. (a) A ring network with ten nodes, and (b) a 5×5 grid with 25 nodes. Node colours indicate community assignments according to Infomap, node sizes illustrate node importance according to map equation centrality based on the shown community structure.

centrality scores.

C. Evaluation setup for empirical networks

We follow previous approaches to evaluate map equation centrality and test how accurately it identifies influential nodes in a network using a discrete-time SIR disease spreading simulation [11]. To estimate a node u 's influence, we calculate its spreading power, that is the expected number of nodes that will be infected by a disease with initial spreader u : Initially, the only infected node is u , all other nodes begin in the susceptible state, and the recovery time is set to 1 time step. As long as there are infected nodes, the simulation continues: infected nodes infect their susceptible neighbours independently with probability p_{th} , then they recover. Here, p_{th} is the so-called epidemic threshold with $p_{\text{th}} = \frac{\langle k \rangle}{\langle k^2 \rangle - \langle k \rangle}$ where $\langle k \rangle = \frac{1}{|V|} \sum_{v \in V} k_v$ and $\langle k^2 \rangle = \frac{1}{|V|} \sum_{v \in V} k_v^2$ are the first and second moment of the network's degree sequence, respectively [18]. When no infected nodes are left, the simulation ends, and we determine u 's spreading power as the number of recovered nodes. Because of the stochasticity in the SIR model, we repeat the simulation 1000 times per node to calculate its expected spreading power.

Let M_c and M_{SIR} be the lists of nodes, ranked according to centrality score c , and their spreading power as determined with the SIR simulation, respectively. Then, we measure the ability of centrality score c to identify influential spreaders using the so-called imprecision function, $\epsilon_c(x) = 1 - \frac{M_c(x)}{M_{\text{SIR}}(x)}$ [19]. Here, $M_c(x)$ and $M_{\text{SIR}}(x)$ are the average spreading power of the top x -fraction of nodes according to centrality score c and the SIR simulation, respectively. A smaller imprecision value corresponds to a better alignment between centrality score c

and spreading power.

D. Empirical Networks

We use eight real-world networks, retrieved from netzscheuler [20], to evaluate map equation centrality's performance. Five of the networks are undirected while three are directed.

Facebook friends: undirected network of Facebook friendships, recorded in April 2014, where a link between users A and B means that they are friends on Facebook [21].

Copenhagen: undirected network of Facebook friendships between university students from Copenhagen where a link between users A and B means that they are friends on Facebook [22].

Uni email: directed network of email exchanges at the Rovira i Virgili University in Spain, recorded in 2003, where a link from user A to user B means that user A has sent an email to user B [23].

Ego Facebook: undirected network of Facebook friendships, recorded in 2021, where a link between users A and B means they are friends on Facebook [24].

Facebook organizations: undirected network of Facebook friendships between users working at the same organization where a link between users A and B means that they are friends on Facebook [25].

Physics collaborations: undirected co-authorship network between researchers who have a preprint on arXiv, recorded in May 2014, where a link between researcher A and B means that they have written an arXiv preprint together [26].

PGP: directed network of users in the Pretty-Good-Privacy (PGP) web of trust, recorded in November 2009. A link from user A to user B means that user A trusts user B [27].

Facebook wall: directed network of interactions between Facebook users, recorded in 2009, where a link from user A to user B means that user A has posted on user B's wall [28].

Table II provides details about the networks' size, their number of communities, mixing, as well as their epidemic threshold. We use networkx [29] to extract the largest connected component from the undirected, and the largest weakly connected component from the directed networks for our analyses. Since estimating nodes' spreading power with the SIR simulation disregards link weights, we treat all networks as unweighted.

To infer the networks' community structure, we select the best result from 1000 Infomap runs, that is the partition with the shortest codelength. In our evaluation, we

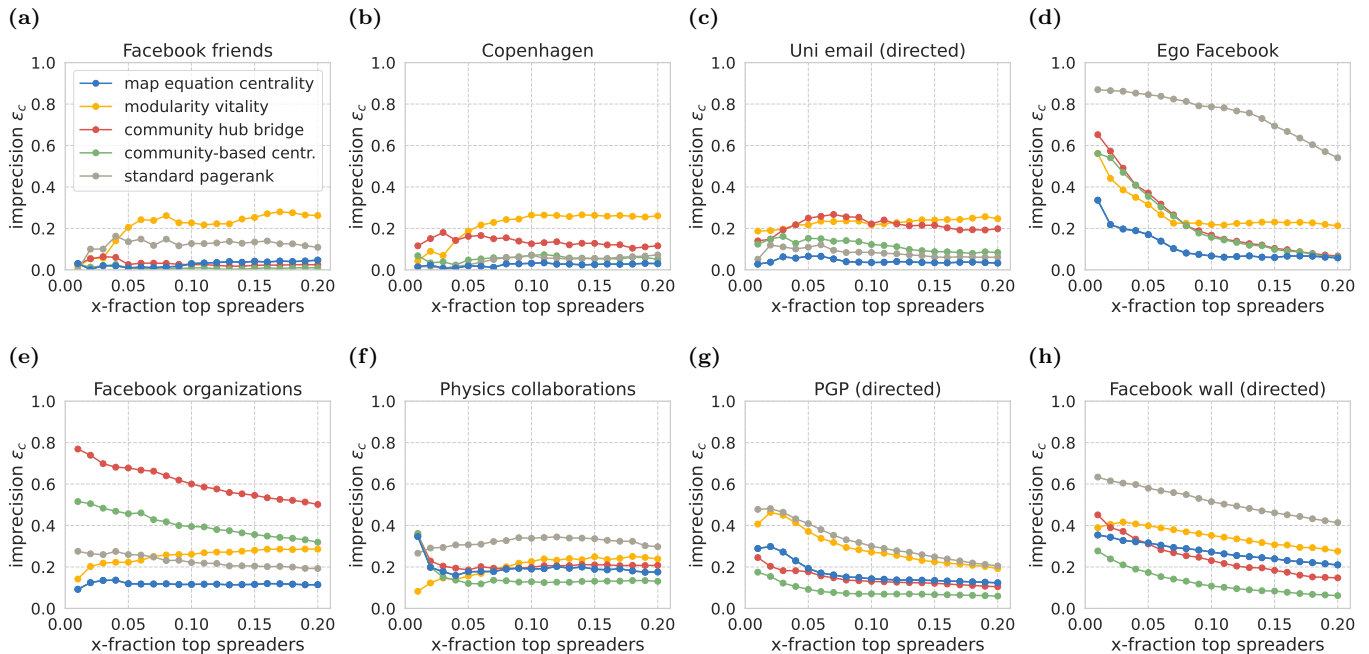


Figure 5: Performance of map equation centrality, modularity vitality, community hub-bridge, community-based centrality, and PageRank for identifying top spreaders in eight empirical networks, based on community structures inferred with Infomap. The curves show imprecision as a function of the x -fraction of top spreaders that are selected according to the five centrality scores. A lower imprecision corresponds to a more accurate identification of top spreaders as determined with an SIR disease spreading simulation.

Table II: List of eight analysed networks with number of nodes, N , number of links, $|E|$, number of communities in the best two-level partition inferred with Infomap, M , mixing, μ , and epidemic threshold, p_{th} . Directed networks are marked with (D) after their name.

Network	N	$ E $	M	μ	p_{th}
Facebook friends	329	1,954	21	0.129	0.048
Copenhagen	800	6,429	36	0.494	0.038
Uni email (D)	1,133	5,452	49	0.396	0.027
Ego facebook	4,039	88,234	76	0.081	0.009
Facebook organizations	5,524	94,219	51	0.356	0.016
Physics collaborations	8,798	27,416	612	0.220	0.066
PGP (D)	39,796	301,498	2870	0.286	0.010
Facebook wall (D)	43,953	271,375	2308	0.483	0.028

consider two-level partitions with non-overlapping communities. We have also tested hierarchical partitions, but did not see a substantial performance difference. For comparison, we include three community-aware centrality scores, modularity vitality [8], community hub-bridge [5], and community-based centrality [6], as well as standard PageRank [3]. Modularity vitality calculates a node u 's importance, given a network G and a partition M , as the difference in modularity between the original network and partition and the network and partition with u re-

moved, $Q(G, M) - Q(G - \{u\}, M - \{u\})$, where Q is the modularity function. Depending on whether deleting a node and its incident edges increases or decreases the partitions modularity, the result can be positive or negative. Following previous evaluations, we consider modularity vitality's absolute value [11]. Community hub-bridge determines a node u 's importance by considering its intra- and inter-community links, weighing them by u 's own community size and the number of other communities it links to, respectively, assigning high importance to nodes with many links in large communities and nodes with many links to a large number of communities, $\sum_{m \in M} |m| \cdot k_u^m + NNC_u \cdot k_u^m$. Here, k_u^m is the number of u 's neighbours in module m , NNC_u is u 's number of neighbouring communities, and $k_u^{\bar{m}}$ is the number of u 's neighbours outside of m . Community-based centrality calculates a node's importance as the number of connections it has to the different communities, weighted by the communities' relative sizes, $\sum_{m \in M} k_u^m \frac{|m|}{N}$. For PageRank, we use the standard teleportation rate of 0.15.

We find that map equation centrality outperforms the four other measures in four of the tested networks, and performs second-to-third best in the other four (Fig. 5). First, in the Facebook friends network, all five measures identify the highest spreading power nodes similarly well while, as we increase the fraction x of top spreaders to be identified, map equation centrality, and community hub-bridge remain nearly tied, followed by

PageRank, and modularity vitality (Fig. 5a). Second, in the Copenhagen network, map equation centrality consistently identifies the top spreader over the investigated x -range. Community-based centrality and PageRank perform similar to map equation centrality up to $x \approx 0.05$ where map equation centrality begins to outperform them. Modularity vitality, while identifying the top spreaders accurately, has worse performance beyond $x = 0.05$. Community hub-bridge shows stable imprecision performance (Fig. 5b). Third, in the Uni email network, map equation centrality outperforms the other measures for all tested x -values, followed by PageRank, community-based centrality, and modularity vitality and community hub-bridge, the latter two performing similarly in this scenario (Fig. 5c). Fourth, in the Ego Facebook network, map equation centrality again outperforms the other measures. Initially and up to $x \approx 0.08$, modularity vitality, community hub-bridge, and community-based vitality show similar performance. Beyond $x \approx 0.08$, modularity vitality’s performance remains stable at an imprecision of around 0.2 while community hub-bridge and community-based centrality improve and perform as well as map equation centrality at $x \approx 0.2$. PageRank performs worse than the other measures in this scenario with imprecision values roughly between 0.9 down to 0.5 (Fig. 5d). Fifth, in the Facebook organizations network, map equation centrality outperforms the other measures with a stable imprecision around 0.1. Modularity vitality and PageRank initially perform second- and third-best, respectively, with PageRank beginning to increasingly outperform modularity vitality from $x \approx 0.07$. Community-based centrality and community hub-bridge perform second-worst and worst, respectively, making this the only tested scenario where they perform worse than the other measures (Fig. 5e). Sixth, in the physics collaborations network, initially modularity vitality performs best, but shows decreasing performance as x increases. PageRank initially performs second-best and shows a similar performance across the whole range of tested x -values. Map equation centrality, community hub-bridge, and community-based centrality initially perform worst, all with an imprecision of around 0.35, but outperform PageRank beyond $x \approx 0.015$, and begin to increasingly outperform modularity vitality beyond $x \approx 0.08$, with community-based centrality performing best (Fig. 5f). Seventh, in the PGP network, community-based centrality outperforms the other measures. Community hub-bridge initially performs second-best, followed by map equation centrality, modularity vitality, and finally PageRank. However, from $x \approx 0.05$, community hub-bridge and map equation centrality are nearly tied, likewise modularity vitality and PageRank perform similarly beyond $x = 0.02$ (Fig. 5g). Eighth, and finally, in the Facebook wall network, community-based centrality outperforms the other measures. Initially, map equation centrality performs second-best, followed by modularity vitality, community hub-bridge, and then PageRank. Beyond $x \approx 0.05$, com-

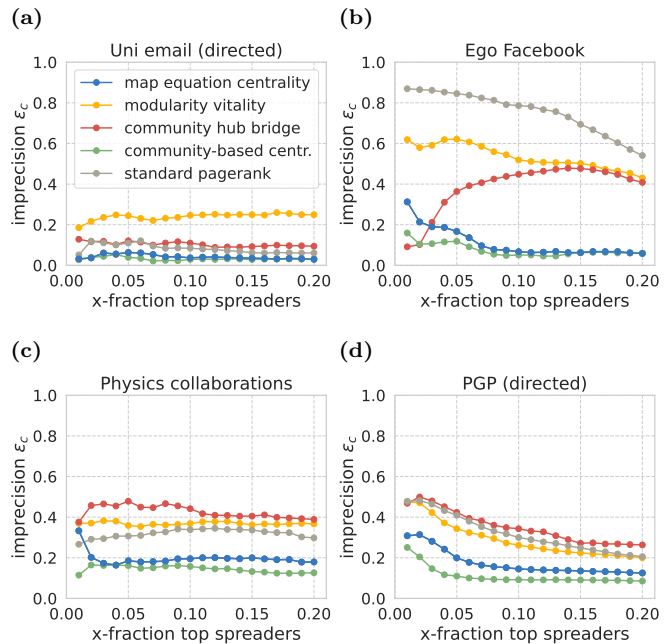


Figure 6: Performance of map equation centrality, modularity vitality, community hub-bridge, community-based centrality, and PageRank for identifying top spreaders in four empirical networks based on partitions inferred with the Leiden algorithm and modularity maximisation.

munity hub-bridge outperforms map equation centrality, and modularity vitality are in fourth, and PageRank in fifth place, respectively (Fig. 5h).

To investigate whether map equation centrality is at an unfair advantage because it is by definition faithful to the map equation, we have repeated our experiments in four of the networks with partitions based on modularity maximisation. To infer the community structure in the Uni email, Ego Facebook, Physics collaborations, and PGP networks, we run the Leiden algorithm [30] 1000 times, and proceed with the partition that has the highest modularity score. As before, we calculate imprecision scores based on how well the five centrality measures identify the top-spreading nodes in the network; the results are shown in Fig. 6. Overall, we find that the new partitions do not affect map equation centrality much, but surprisingly, modularity vitality performs worse compared to when the partitions were based on the map equation. Community hub-bridge performs worse than before while community-based centrality performs better under the modularity-based partitions. In contrast to the community-aware centrality scores, PageRank is entirely unaffected by the choice of community structure because it does not rely on a network partition to compute centrality scores. Whereas map equation centrality remains the best-performing score in the Uni email network (Fig. 6a), community-based centrality now outperforms map equation centrality in the Ego

Facebook network (Fig. 6b). In the Physics collaborations and the PGP networks, the situation remains as before with community-based centrality performing best, followed by map equation centrality (Fig. 6c, Fig. 6d).

To summarise, we found that none of the tested centrality scores outperforms all other scores in all networks, neither did we find a score that performed worst in all cases. However, map equation centrality outperformed modularity vitality, community hub-bridge, community-based centrality, and PageRank in half of the networks while performing second-to-third best in the other half.

V. CONCLUSION

We have studied node importance from a community-detection perspective within the map equation framework and analytically derived a community-aware centrality score. Our score exploits modular network structure and assigns centrality scores to nodes based on their community embedding; to determine a node's centrality, it suffices to consider those nodes that belong to the same community. In contrast, traditional centrality mea-

asures typically neglect local network structure and rely on node features or global patterns to determine node importance instead. Community-aware centrality measures are often defined in an ad-hoc way, disconnected from the assumptions made by community-detection methods. In contrast, map equation centrality is true to the map equation. We have highlighted how map equation centrality discerns nodes indistinguishable to global centrality measures using a synthetic network and pointed out its limitations by considering networks without community structure. On a set of eight real-world networks, map equation centrality tends to outperform baseline methods in identifying influential nodes.

ACKNOWLEDGMENTS

We would like to thank Anton Eriksson for helping with implementing map equation centrality in Infomap. This work was partially supported by the Wallenberg AI, Autonomous Systems and Software Program (WASP) funded by the Knut and Alice Wallenberg Foundation. Martin Rosvall was supported by the Swedish Research Council, Grant No. 2016-00796.

-
- [1] D. Koschützki, K. A. Lehmann, L. Peeters, S. Richter, D. Tenfelde-Podehl, and O. Zlotowski, Centrality indices, in *Network analysis* (Springer, 2005) pp. 16–61.
 - [2] L. Katz, A new status index derived from sociometric analysis, *Psychometrika* **18**, 39 (1953).
 - [3] D. F. Gleich, Pagerank beyond the web, *SIAM Rev.* **57**, 321–363 (2015).
 - [4] M. Kitromilidis and T. S. Evans, Community detection with metadata in a network of biographies of western art painters (2018), [arXiv:1802.07985 \[physics.soc-ph\]](https://arxiv.org/abs/1802.07985).
 - [5] Z. Ghalmane, M. El Hassouni, and H. Cherifi, Immunization of networks with non-overlapping community structure, *Social Network Analysis and Mining* **9**, 1 (2019).
 - [6] Z. Zhao, X. Wang, W. Zhang, and Z. Zhu, A community-based approach to identifying influential spreaders, *Entropy* **17**, 2228 (2015).
 - [7] Z. Ghalmane, M. El Hassouni, C. Cherifi, and H. Cherifi, Centrality in modular networks, *EPJ Data Science* **8**, 15 (2019).
 - [8] T. Magelinski, M. Bartulovic, and K. M. Carley, Measuring node contribution to community structure with modularity vitality, *IEEE Transactions on Network Science and Engineering* **8**, 707 (2021).
 - [9] M. E. J. Newman and M. Girvan, Finding and evaluating community structure in networks, *Phys. Rev. E* **69**, 026113 (2004).
 - [10] M. Rosvall and C. T. Bergstrom, Maps of random walks on complex networks reveal community structure, *Proc. Natl. Acad. Sci. U.S.A.* **105**, 1118 (2008).
 - [11] S. Rajeh, M. Savonnet, E. Leclercq, and H. Cherifi, Comparing community-aware centrality measures in online social networks, in *Computational Data and Social Networks*, edited by D. Mohaisen and R. Jin (Springer International Publishing, Cham, 2021) pp. 279–290.
 - [12] C. E. Shannon, A mathematical theory of communication, *Bell Labs Tech. J.* **27**, 379 (1948).
 - [13] R. Lambiotte and M. Rosvall, Ranking and clustering of nodes in networks with smart teleportation, *Phys. Rev. E* **85**, 056107 (2012).
 - [14] D. Edler, L. Bohlin, and M. Rosvall, Mapping Higher-Order Network Flows in Memory and Multilayer Networks with Infomap, *Algorithms* **10**, 112 (2017).
 - [15] D. Edler, A. Eriksson, and M. Rosvall, *The Infomap Software Package* (2020).
 - [16] S. Fortunato and M. Barthelemy, Resolution limit in community detection, *Proceedings of the national academy of sciences* **104**, 36 (2007).
 - [17] T. Kawamoto and M. Rosvall, Estimating the resolution limit of the map equation in community detection, *Phys. Rev. E* **91**, 012809 (2015).
 - [18] W. Wang, Q.-H. Liu, L.-F. Zhong, M. Tang, H. Gao, and H. E. Stanley, Predicting the epidemic threshold of the susceptible-infected-recovered model, *Scientific reports* **6**, 1 (2016).
 - [19] M. Kitsak, L. K. Gallos, S. Havlin, F. Liljeros, L. Muchnik, H. E. Stanley, and H. A. Makse, Identification of influential spreaders in complex networks, *Nature physics* **6**, 888 (2010).
 - [20] T. P. Peixoto, The netzscheuler network catalogue and repository, <https://networks.skewed.de/> (2020).
 - [21] B. F. Maier and D. Brockmann, Cover time for random walks on arbitrary complex networks, *Phys. Rev. E* **96**, 042307 (2017).
 - [22] P. Sapiezynski, A. Stopczynski, D. D. Lassen, and S. Lehmann, Interaction data from the copenhagen networks study, *Scientific Data* **6**, 1 (2019).

- [23] R. Guimerà, L. Danon, A. Díaz-Guilera, F. Giralt, and A. Arenas, Self-similar community structure in a network of human interactions, *Phys. Rev. E* **68**, 065103 (2003).
- [24] J. Mcauley and J. Leskovec, Discovering social circles in ego networks, *ACM Transactions on Knowledge Discovery from Data (TKDD)* **8**, 1 (2014).
- [25] M. Fire and R. Puzis, Organization mining using online social networks, *Networks and Spatial Economics* **16**, 545 (2016).
- [26] M. De Domenico, A. Lancichinetti, A. Arenas, and M. Rosvall, Identifying modular flows on multilayer networks reveals highly overlapping organization in interconnected systems, *Phys. Rev. X* **5**, 011027 (2015).
- [27] O. Richters and T. P. Peixoto, Trust transitivity in social networks, *PLoS one* **6**, e18384 (2011).
- [28] B. Viswanath, A. Mislove, M. Cha, and K. P. Gummadi, On the evolution of user interaction in facebook, in *Proceedings of the 2nd ACM workshop on Online social networks* (2009) pp. 37–42.
- [29] A. A. Hagberg, D. A. Schult, and P. J. Swart, Exploring network structure, dynamics, and function using networkx, in *Proceedings of the 7th Python in Science Conference*, edited by G. Varoquaux, T. Vaught, and J. Millman (Pasadena, CA USA, 2008) pp. 11 – 15.
- [30] V. A. Traag, L. Waltman, and N. J. Van Eck, From louvain to leiden: guaranteeing well-connected communities, *Scientific reports* **9**, 1 (2019).

Appendix A: Generalisation to sets

We generalise map equation centrality and derive the expression in Eq. 12 that can be used to calculate the combined centrality for sets of nodes U . We follow the same approach as before, that is, we first derive an expression for the expected per-step codelength when silencing all nodes in U while using the old coding scheme; then we derive an expression for the expected per-step codelength when designing a new coding scheme that does not assign codewords to nodes in U to start with.

Let $G = (V, E, \delta)$ be a graph with nodes V , links E , weights δ , $U \subseteq V$ be a set of nodes, and $p_U = \sum_{u \in U} p_u$ be the visit rate sum of nodes in U . Further, for a module m , let $p_{m \cap U} = \sum_{u \in m \cap U} p_u$ be the visit rate sum of nodes that are members in m and in U , and let $P_{m \cap U} = \{p_u \mid u \in m \cap U\}$ be their set of visit rates.

We begin with the one-level partition M_1 and obtain the expected per-step codelength for describing a random walk with nodes in U silenced while using the old coding scheme. Removing the silenced nodes from the summation in Eq. 1, we get

$$L^U(G, M_1) = - \sum_{v \in V \setminus U} p_v \log_2 p_v. \quad (\text{A1})$$

We obtain the codelength for a new coding scheme that does not assign codewords to nodes in U by normalising the visit rates for the remaining nodes with

$$1 - p_U,$$

$$L^{U*}(G, M_1) = - \sum_{v \in V \setminus U} p_v \log_2 \frac{p_v}{1 - p_U}. \quad (\text{A2})$$

The difference between Eq. A1 and Eq. A2 is the joint map equation centrality score of the nodes in U under M_1 ,

$$\begin{aligned} \lambda(G, M_1, U) &= L^U(G, M_1) - L^{U*}(G, M_1) \\ &= -(1 - p_U) \log_2 (1 - p_U). \end{aligned} \quad (\text{A3})$$

For two-level partitions, we begin by rewriting the map equation (Eq. 2) to distinguish explicitly between modules that have an overlap with U and those that do not,

$$\begin{aligned} L(G, M) &= \quad (\text{A4}) \\ &\overbrace{qH(Q)}^{\text{index level}} + \overbrace{\sum_{\substack{m \in M \\ m \cap U = \emptyset}} p_m H(P_m)}^{\text{no overlap with } U} - \overbrace{\sum_{\substack{m \in M \\ m \cap U \neq \emptyset}} \sum_{p \in P_m} p \log_2 \frac{p}{p_m}}^{\text{overlap with } U}. \end{aligned}$$

The codelength for describing a random walk in partition M with nodes in U silenced when using the old coding scheme is

$$\begin{aligned} L^U(G, M) &= \quad (\text{A5}) \\ &\overbrace{qH(Q)}^{\text{index level}} + \overbrace{\sum_{\substack{m \in M \\ m \cap U = \emptyset}} p_m H(P_m)}^{\text{no overlap with } U} - \overbrace{\sum_{\substack{m \in M \\ m \cap U \neq \emptyset}} \sum_{p \in P_m \setminus P_{m \cap U}} p \log_2 \frac{p}{p_m}}^{\text{overlap with } U}. \end{aligned}$$

With a new code that does not assign codewords to nodes in U and that normalises accordingly, the codelength is

$$\begin{aligned} L^{U*}(G, M) &= \overbrace{qH(Q)}^{\text{index level}} + \overbrace{\sum_{\substack{m \in M \\ m \cap U = \emptyset}} p_m H(P_m)}^{\text{no overlap with } U} \\ &- \overbrace{\sum_{\substack{m \in M \\ m \cap U \neq \emptyset}} \sum_{p \in P_m \setminus P_{m \cap U}} p \log_2 \frac{p}{p_m - p_{m \cap U}}}^{\text{overlap with } U}. \end{aligned} \quad (\text{A6})$$

The difference between Eq. A5 and Eq. A6 is the joint map equation centrality of the nodes in U under M ,

$$\begin{aligned} \lambda(G, M, U) &= L^U(G, M) - L^{U*}(G, M) \quad (\text{A7}) \\ &= - \sum_{m \in M, m \cap U \neq \emptyset} (p_m - p_{m \cap U}) \log_2 \frac{p_m - p_{m \cap U}}{p_m}. \end{aligned}$$